SEMITRANSPARENT ZnO/PEDOT BASED HYBRID INORGANIC/ORGANIC HETEROJUNCTION THIN FILM DIODES PREPARED BY COMBINED RF MAGNETRON SPUTTERING AND ELECTRODEPOSITION TECHNIQUES.

Jorge Rodríguez-Moreno[1], Elena Navarrete-Astorga[1], Francisco Martín[1], Ricardo Schrebler[2], José R. Ramos-Barrado[1], Enrique A. Dalchiele[3]

[1]*Laboratorio de Materiales y Superficies (Unidad Asociada al CSIC). Departamentos de Física Aplicada & Ing. Química, Universidad de Málaga, E29071 Málaga, Spain.*

[2]*Instituto de Química, Facultad de Ciencias, Pontificia Universidad Católica de Valparaíso, Casilla 4059, Valparaíso, Chile.*

[3]*Instituto de Física, Facultad de Ingeniería, Herrera y Reissig 565, C.C. 30, 11000 Montevideo, Uruguay.*

Number of pages:	*22, including title page, abstract, main text, references, figure captions and figures.*
Number of tables:	*1*
Number of figures:	*6*
Running title:	*"ZnOPedot"*

Please address correspondence related to this paper to: Enrique A. Dalchiele, dalchiel@fing.edu.uy , Tel. ++598-2-7110905, Montevideo, Uruguay.

Highlights

- ✓ n-ZnO/p-PEDOT semitransparent inorganic-organic hybrid vertical heterojunction thin film diodes have been fabricated with PEDOT and ZnO thin films grown by electrodeposition and RF magnetron sputtering respectively.
- ✓ The diode exhibited an optical transmission of ~40% to ~50% in the visible region between 450 and 700 nm.
- ✓ The current-voltage (I-V) characteristics of the heterojunction show good rectifying diode characteristics, with a ratio of forward current to the reverse current as high as 35 in the range -4 V to +4 V.

SEMITRANSPARENT ZnO/PEDOT BASED HYBRID INORGANIC/ORGANIC HETEROJUNCTION THIN FILM DIODES PREPARED BY COMBINED RF MAGNETRON SPUTTERING AND ELECTRODEPOSITION TECHNIQUES.

Jorge Rodríguez-Moreno[1], Elena Navarrete-Astorga[1], Francisco Martín[1], Ricardo Schrebler[2], José R. Ramos-Barrado[1], Enrique A. Dalchiele[3]

[1]*Laboratorio de Materiales y Superficies (Unidad Asociada al CSIC). Departamentos de Física Aplicada & Ing. Química, Universidad de Málaga, E29071 Málaga, Spain.*

[2]*Instituto de Química, Facultad de Ciencias, Pontificia Universidad Católica de Valparaíso, Casilla 4059, Valparaíso, Chile.*

[3]*Instituto de Física, Facultad de Ingeniería, Herrera y Reissig 565, C.C. 30, 11000 Montevideo, Uruguay.*

Number of pages:	*22, including title page, abstract, main text, references, figure captions and figures.*
Number of tables:	*1*
Number of figures:	*6*
Running title:	*"ZnOPedot"*

Please address correspondence related to this paper to: Enrique A. Dalchiele, dalchiel@fing.edu.uy , Tel. ++598-2-7110905, Montevideo, Uruguay.

Abstract. n-ZnO/p-PEDOT semitransparent inorganic-organic hybrid vertical heterojunction thin film diodes have been fabricated with PEDOT and ZnO thin films grown by electrodeposition and RF magnetron sputtering respectively, onto an ITO/glass substrate. The diode exhibited an optical transmission of ~40% to ~50% in the visible region between 450 and 700 nm. The current-voltage (I-V) characteristics of the heterojunction show good rectifying diode characteristics, with a ratio of forward current to the reverse current as high as 35 in the range -4 V to +4 V. The I-V characteristic was examined in the framework of the thermionic emission model. The ideality factor and barrier height were obtained as 4.0 and 0.88 eV respectively.

Keywords: Semitransparent heterojunction; n-ZnO; PEDOT; sputtering; electrodeposition.

1. INTRODUCTION

In the last years, transparent electronics (i.e.: transparent diodes, functional windows, TFT, CMOS, etc.), becomes an important and emerging area of advanced technology research [1]. However, although the n-type transparent conductive oxides (TCOs) such as ZnO, In_2O_3, SnO_2 and their doped versions are well-known and widely used in many opto-electronic applications, transparent devices based on the transparent p-n junctions are limited to the scarce existence of p-type TCOs [1-3]. On the other hand, a p-type conducting polymer as the poly(3,4-ethylenedioxythipohene) (PEDOT) doped with poly(styrenesulfonic acid) (PEDOT:PSS), has attracted considerable interest in recent years because for its low-energy band gap (ca. 1.6-1.7) which makes it suitable for electro-optical applications, its excellent electrical characteristics, inherent stability and low oxidation potential [4]. In fact, PEDOT is being widely employed in organic photovoltaic devices and organic light-emitting diodes (OLEDs) as hole transporting layer, because of its suitable work function and acceptable transparency in visible light range [5-10]. Moreover, several pioneering studies showing the possibilities of ZnO/PEDOT:PSS based hybrid inorganic/organic heterostructures in optoelectronic and photovoltaic devices such as diodes [9,11-14] and solar cells [5] have been emerged. Hybrid inorganic/organic heterostructures have been shown to posses a great potential in optoelectronic and photovoltaic devices [5,15-19]. In fact, the hybrid structures can combine in one assembly the advantages of inorganic compounds such as a broad range of light absorption, effective transport of charge carriers, firmness, hardness, and thermo-stability, and advantages of organic polymer materials such as cheapness, plasticity, flexibility, easy chemical modification, and solution processibility [5,16]. In the case of ZnO/PEDOT:PSS based hybrid inorganic/organic heterostructures, different ZnO architectures (planar single crystal [11], thin films [14] and nanowires [9,12,13]),

and several preparation techniques for both ZnO structures and PEDOT:PSS layers in fabricating those mentioned heterostructured devices can be encountered in the literature. In the PEDOT:PSS film preparation, as a general rule in all those cases above mentioned, a spin coating technique has been used [9,11-14]. In the case of the literature reported ZnO thin film/PEDOT:PSS heterojunction diode, the ZnO thin film has been grown by an ultrasonically assisted chemical vapor deposition technique [14].

In this contribution, the fabrication of n-ZnO/p-PEDOT based hybrid inorganic/organic semitransparent heterostructure diodes has been performed by using an innovative combined physical magnetron sputtering growth method and a low-cost electrochemical one. The first step consists of the growth of the PEDOT thin film by an electrochemical route through the electropolymerization of EDOT monomer from an organic electrolyte solution onto an ITO-coated glass substrate. In a second step a ZnO thin film is deposited by magnetron sputtering method onto the previously electrochemically grown PEDOT layer. Thus, producing through low temperature processes a hybrid inorganic/organic heterostructure. It is noteworthy that the low temperature processing may allow for preparing optoelectronic devices and solar cells onto flexible plastic substrates [10], and then providing an opportunity to bring new applications in wearable computers, flexible displays, e-papers, electronic textiles, and solar cells. Moreover, in this research, the I-V diode characteristics of the n-ZnO/p-PEDOT device have been investigated.

2. EXPERIMENTAL

Synthesis of ZnO/PEDOT/ITO/glass heterojunction. The first step consists of the growth of the PEDOT thin film by an electrochemical route through the electropolymerization of the (3,4-ethylene dioxythiophene) (EDOT) monomer

(SIGMA-ALDRICH), onto a tin-doped indium oxide (ITO)-coated glass substrate. A typical three electrode electrochemical cell geometry has been used, comprising an ITO-coated glass substrate (2.0 cm^2), a Pt wire and a saturated calomel electrode (SCE) (E=+0.25V vs. normal hydrogen electrode (NHE)), as working, counter and reference electrodes, respectively. All the potentials reported in this study refer to this reference electrode. The electrodeposition bath consisted of an aqueous solution of 3 mM EDOT + 0.2 M $LiClO_4$. All solutions were prepared from analytical grade reagents and 18.3 MΩ.cm Millipore water. The electrodeposition was performed at room temperature. Nitrogen was flushed through the cell and the electrolyte prior to the experiments, and a nitrogen flow was maintained over the solution during the electrodeposition process. The substrates were first cleaned under ultrasonic, 5 min in acetone, 5 min in ethanol and 5 min in DI water. The PEDOT thin film has been grown by a potential cycling procedure between -0.8 to 2 V at 75mV/s, during 5 cycles, by using an Autolab PGSTAT30 potentiostat/galvanostat. In a second step, a ZnO thin film has been grown onto the previously electrodeposited PEDOT layer by RF magnetron sputtering, at room temperature, for 30 minutes by using a Magnetron Sputtering System ORION-5-UHV (AJA International). A ZnO tablet target (99.99% AJA International 2" diameter x 0.125" thickness) has been employed. During deposition, the chamber pressure and RF power have been kept at $1.4x10^{-2}$ mbar and 150 W, respectively. The last step in the fabrication of the hybrid heterojunction diode was the fabrication of a top metal contact to the ZnO part of the hybrid junction. This ohmic contact was achieved by sputtering an Al film through a mask on top of the fabricated device.

Characterization studies. The morphology of the different films has been investigated with a SEM-FIB, FEI-Helios 650 at an acceleration voltage of 3kV. The X-ray diffraction (XRD) of the sputtered ZnO thin film was recorded using Philips X'Pert

PRO MPD unit (with 45kV and 40mA, Cu Kα radiation with λ=1.5406Å). FT-IR spectra of PEDOT thin films were obtained by using a VERTEX 70 spectrophotometer with a Golden Gate Single Reflection Diamond ATR System from Specac. The optical properties of the diode devices in the visible spectral region have been studied by a Spectrometer Varian Cary 5000 (180 to 3300 nm) with an integrating Sphere and variable angle. The thickness and roughness of the films have been determined by using a mechanical profilometer DEKTAK 150 SURFACE PROFILER from Veeco. A potentiostat/galvanostat Autolab PGSTAT30 was used to measure the I-V characteristics of the devices. All measurements were performed at room temperature and in dark conditions.

3. RESULTS AND DISCUSSION

Properties of PEDOT and ZnO thin films

The PEDOT thin films onto the ITO substrate have been obtained through the electropolymerization of the EDOT monomer in an aqueous $LiClO_4$ solution. The electropolymerization has been carried out potentiodynamically by cycling the potential from -0.8 to 2.0 V. After five cycles the as-deposited PEDOT thin films exhibited a light blue color and good transparency, were uniform with no visible defects and they had good adhesion to the ITO surface. The thickness of the electropolymerized PEDOT layer can easily be controlled by the deposition time, which in the case of potential cycling is number of cycles. After five cycles, a final PEDOT film thickness of about 200 nm has been obtained, as it was determined by profilometric analysis. Moreover, this film thickness value is in accordance to the one (ca. 220 nm), obtained from the

polymerization charge and applying the Faraday's law (assuming a 100% Faradaic efficiency).

In order to quantitatively confirm that the electrodeposited thin films were PEDOT, FTIR-ATR spectroscopy has been carried out onto those thin films. Figure 1 shows the FTIR-ATR spectrum in the wavenumber region 1600-800 cm^{-1} of a typical electrodeposited PEDOT thin film. In this FTIR-AR spectrum 11 peaks can be assigned to PEDOT (see Table 1), showing conclusively that the electrodeposited thin films are composed of PEDOT. Moreover, the presence of strong signal bands at ca. 1520 cm^{-1} and at ca. 1360 cm^{-1} demonstrates that the electrochemically grown PEDOT films are p-doped [22].

Figure 2 shows FE-SEM images of a typical PEDOT layer electrochemically grown under the experimental conditions described above. Figure 2a depicts a continuous and homogenous film, without cracks or pinholes. With a higher magnification, Fig. 2b shows a rough granular layer of round-shaped particles about 250 nm in diameter. The layer is dense with a relatively low roughness of ca. 10 nm as determined by profilometry. Despite high surface area the roughness stays on the level of 10 nm, preventing electrical pinning [23].

As has been said above in a second step a ZnO thin film has been deposited onto the previously electrochemically grown PEDOT layer by RF magnetron sputtering. The ZnO film thickness was of about 700 Å. The ZnO film surface was smooth, homogenous and without cracks. In order to study the structural properties of the ZnO films, i.e.: to investigate the crystallographic phase, the overall crystalline quality, and the possible texture of those ZnO grown thin films, X-ray diffraction experiments have been carried out. Figure 3 shows a typical XRD pattern for sputtered ZnO thin films,

and for comparison its respective JCPDS pattern is also included [24]. The diffractogram revealed a number of diffraction peaks arising from ZnO thin film and ITO substrate layer. The presence of only one diffraction peak corresponding to the (0002) plane of the ZnO wurzite structure can be appreciated, indicating that these films are single-phase with an excellent preferential crystallographic orientation in the c-axis direction. On the other hand, the low intensity of the ZnO diffraction peak compared to the ITO ones is an indication of the low thickness of the films and/or a very low crystalline character.

Optical properties of n-ZnO/p-PEDOT heterojunction diode

In order to investigate the transparency properties of the hybrid heterojunction diode optical transmittance measurements have been done. Figure 4 shows the cumulative optical transmittance versus wavelength spectra of the ZnO/PEDOT/ITO/glass heterojunction thin film diode. Curve (a) and curve (b) represents the transmission spectra of glass and ITO/glass substrate respectively, showing each of them almost 90% and 80% visible transmittance, respectively. The cumulative optical transmittance after depositing each multilayer shows 54% for PEDOT onto ITO/glass substrate (curve (c)), and the final cumulative transmittance of the diode reveals 45% at 550 nm (curve (d)), respectively. Moreover, curve (d) shows an optical transmission of ~40% to ~50% in the visible region between 450 and 700 nm. This compares to an optical transmission in the visible of ca. 30%-60% reported by Lee et al. [25] for their thin film based pentacene/ZnO p-n heterojunction diode and 10% to 55% transmittance reported by Zhou et al. [26] for their glass/PH1000/ZnO/P3HT:$PC_{60}BM$/CPP-PEDOT/PH1000 hybrid organic/inorganic

heterojunction diodes in the visible region. As far as other transparent diodes are concerned, Wang et al. [27] obtained 10% to 70% visible transmittance for n-ZnO/p-type diamond thin films heterojunction diodes, Banerjee et al. [2] reported ca. 60% visible transmittance in a n-$Zn_{1-x}Al_xO$/p-$CuAlO_{2+x}$ heterojunction diode, and Hoffman et al. [28] obtained 35% to ca. 65% for their $CuYO_2$:Ca/ZnO:Al/ITO p-i-n heterojunction diode.

Electrical properties of n-ZnO/p-PEDOT diode

The device structure is illustrated in Fig. 5a. It is a ZnO/PEDOT vertical n-p junction diode with ITO and aluminum (Al) metal as the bottom and top electrodes, respectively. The junction properties were examined by current-voltage (I-V) measurements at room temperature in air under dark conditions. Prior to examining the rectifying properties of the heterojunction diode, it is necessary to confirm ohmic behaviors of the electrodes. Figure 5b depicts an energy band diagram of the n-ZnO/p-PEDOT device constructed in the basis of work function values, PEDOT HOMO and LUMO positions and ZnO data reported in literature [14,15,25, 29-31]. As has been said above and illustrated in the schematic of the device structure (see Fig. 5a), the ITO electrode is used as ohmic contact for p-type PEDOT layer and the Al electrode is used for the ohmic contact for n-type ZnO thin film. The work function of ITO ($\Phi_{ITO} \approx 4.8$ eV) and PEDOT ($\Phi_{PEDOT} \approx 5.0$ eV) are similar, leading to the formation of an ohmic contact. In fact, the linearity of the I-V characteristic of the ITO/PEDOT structure shown in the inset of Fig. 6a, indicates and confirms the ohmic behavior between the ITO/PEDOT. Concerning the Al/ZnO contact, there is also not much difference in the work function of Al ($\Phi_{Al} \approx 4.3$ eV) and the electron affinity of ZnO ($\chi_{ZnO} \approx 4.5$ eV),

leading to ohmic contact at this interface. Furthermore, aluminum has been extensively proved and reported as an ohmic contact material for n-ZnO [32]. Figure 6a shows the current-voltage (I-V) characteristic of a typical n-ZnO/p-PEDOT heterostructure diode. The current increases non-linearly with the forward bias which confirms a diode-like behavior due to difference in energy levels of PEDOT and ZnO thin films [14]. The device shows a low turn-on voltage of approximately 0.5 V under forward bias, in line with the one reported for a PEDOT:PSS/ZnO thin film based diode by Sharma et al. [14]. On the other hand, this turn-on voltage (V_{on}) value is better than those reported for Ga-doped ZnO/PEDOT:PSS (V_{on}=1.3 V) [33] and ZnO/PEDOT:PSS (V_{on}=1.0 V) [34] heterojunction diodes. Moreover, the junction shows a good diode rectifying behavior: the DC rectification ratio |I(4 V)| /| I(-4 V)| is ca. 35. A rectification factor that is comparable to that exhibited by other hybrid inorganic/organic diodes, i.e.: 3.8 at ±5 V for a n-ZnO nanorod arrays/p-PEDOT:PSS heterojunction [16], 50 at ±3 V for a Ga-doped ZnO/PEDOT:PSS device [33], 25 at ±5 V for a ZnO nanowire arrays/PEDOT:PSS diode device [13] and 16 at ± 5 V for a ZnO/polyaniline heterostructure [15].

The diode-like behavior of the n-ZnO/p-PEDOT heterojunction was examined using thermionic emission model [35]. According to this model, the junction under forward bias has the I-V relation as:

$$I = I_S\left[\exp\left(\frac{qV}{nkT}\right)-1\right] \qquad (V \geq 3k_BT/q), \qquad (1)$$

where V is the applied bias voltage (in V), I is the measured current, I_S is the saturation current, q is the absolute value of the electronic charge (in C), k and T are Boltzmann's constant and absolute temperature, respectively, n is the ideality factor (in the ideal case

n=1, if the transport mechanism is not governed exclusively by a thermionic emission process, n>1). The saturation current I_S is expressed as:

$$I_S = AA^*T^2 \exp\left(-\frac{q\Phi_b}{kT}\right) \qquad (2)$$

where A is the junction area, A* is the effective Richardson constant and Φ_b is the barrier height at the ZnO/PEDOT interface. The slope and the intercept from the linear fit to the semilog plot of the I-V curve depicted in Fig. 6b yield the ideality factor, n=4.0, and the barrier height, Φ_b=0.88 eV. The resultant ideality factor value is similar to the reported n value (3.8), for a CVD deposited ZnO/spin coated PEDOT:PSS n-p thin film based diode [14]. This ideality factor is expected to be 1.0 and 2.0 at low and higher voltage, respectively, as per the classic Sah-Noyce-Shockley model [36]. The high n value elucidates that the behavior of the ZnO/PEDOT junction diode deviates from the ideal one. This may be due to the presence of surfaces states in ZnO as has been suggested by several authors [14,34], and interface states at the inorganic/polymer heterostructure interface [34, 37].

4. CONCLUSIONS

n-ZnO/p-PEDOT semitransparent inorganic-organic hybrid vertical heterojunction thin film diodes have been fabricated with PEDOT and ZnO thin films grown by electrodeposition and RF magnetron sputtering respectively, onto an ITO/glass substrate. The diode exhibited an optical transmission of ~40% to ~50% in the visible region between 450 and 700 nm. The current-voltage (I-V) characteristics of the heterojunction show good rectifying diode characteristics, with a ratio of forward current to the reverse current as high as 35 in the range -4 V to +4 V. The I-V

characteristic was examined in the framework of the thermionic emission model. The ideality factor and barrier height were obtained as 4.0 and 0.88 eV respectively. A moderate transparency and low turn-on voltage of the n-ZnO/p-PEDOT transparent diode indicates its potential application in “transparent” or “invisible electronics”.

Acknowledgements.

The authors are grateful to MICINN of Spain, for the financial support received (Consolider Ingenio 2010 FUNCOAT-CSD2008-00023). This work was partially supported by CSIC (Comisión Sectorial de Investigación Científica) of the Universidad de la República, in Montevideo, Uruguay, and PEDECIBA – Física. R.S. thanks the support received by the D.I.-Pontificia Universidad Católica de Valparaíso, Chile.

REFERENCES

[1] S. Kim, H. Seok, H. Lee, M. Lee, D. Choi, K. Chai, Thin Solid Films 515 (2007) 7324.

[2] A.N. Banerjee, S. Nandy, C.K. Ghosh, K.K. Chattopadhyay, Thin Solid Films 515 (2007) 7324.

[3] T. Yang, X. Qin, H. Wang, Q. Jia, R. Yu, B. Wang, J. Wang, K. Ibrahim, X. Jiang, Q. He, Thin Solid Films 518 (2010) 5542.

[4] A. Elschner, W.Lövenich, MRS Bulletin 36 (2011) 794-798.

[5] J. Bouclé, P.Ravirajan, J. Nelson, J. Mater. Chem. 17 (2007) 3141-3153.

[6] K. M. Kim, K. W. Lee, A.Moujoud, S. H. Oh, H. J. Kim, Electrochem. Solid-State Lett.13 (2010) H447.

[7] M. Hsu, P. Yu, J. Huang, C. Chang, C. Wu, Y. Cheng, C. Chu, Appl. Phys. Lett.98 (2011) 073308.

[8] O.P. Dimitriev, V.V. Kislyuk, A.F. Syngaevsky, P.S. Smertenko, A.A. Pud, Phys. Status Solidi A 11 (2009) 2645-2651.

[9] C. Chang, F.Tsao, C. Pan, G. Chi, H. Wang, J. Chen, F. Ren, D.P. Norton, S.J. Pearton, K. Chen, L. Chen, Appl. Phys. Lett. 88 (2006) 173503.

[10] S. Eom, S. Senthilarasu, P.Ulthirakumar, S. C. Yoon, J. L. C. Lee, H. S. Lim, J. Lee, S. Lee, Org. Electron. 10 (2009) 536-542.

[11] M. Nakano, A. Tsukazaki, R. Y. Gunji, K. Ueno, A. Ohtomo, T. Fukumura, M. Kawasaki, Appl. Phys. Lett. 91 (2007) 142113.

[12] C. S. Rout, C N R Rao, Nanotechnol. 19 (2008) 285203.

[13] A. El-Shaer, A.Dev, J.Richters, S. R. Waldvogel, J.Waltermann, W.Schade, T. Voss, Phys. Status Solidi B 6 (2010) 1564-1567.

[14] B. K. Sharma, N.Khare, S. Ahmad, Solid State Commun. 149 (2009) 771-774.

[15] S. Mridha, D. Basak, Appl. Phys. Lett.92 (2008) 142111.

[16] S.Shiu, J. Chao, S. Hung, C.Yeh, C. Lin, Chem. Matter. 22 (2010) 3108-3113.

[17] F. Habelhames, B. Nessark, M. Girtan, Mater. Sci. Semicond. Process. 13 (2010) 141–146.

[18] D. C. Olson, J.Piris, R. T. Collins, S. E. Shaheen, D. S. Ginley, Thin Solid Films 496 (2006) 26-29.

[19] H. Hoppe, N. S.Sariciftci, J. Mater.Res.19 (2004) 1924.

[20] D. K. Taggart. Y. Yang, S. Kung. T. M. McIntire and R. M. Penner, Nano Lett. 11(2011) 125.

[21] M. Döbbelin, R. Tena-Zaera, P.M. Carrasco, J.-R. Sarasua, G. Cabañero, D. Mecerreyes, J. Polym. Sci., Part A: Polym. Chem. 48 (2010) 4648.

[22] C. Kvarnström, H. Neugebauer, A. Ivaska and N.S. Sariciftci, Journal of Molecular Structure 521 (2000) 271–277.

[23] E. Nasybulin, S. Wei, M. Cox, I. Kymissis and K. Levon, J. Phys. Chem. C 115 (2011) 4307.

[24] Powder Diffraction File, Joint Committee for Powder Diffraction Studies (JCPDS) File No. 05-0664 (hexagonal structure of ZnO).

[25] K.H. Lee, C.H. Park, K. Lee, T. Ha, J.H. Kim, J. Yun, G-H. Lee, S. Im, Org. Electron. 12 (2011) 1103.

[26] Y. Zhou, H. Cheun, S. Choi, W.J. Potscavage, C. Fuentes-Hernandez, B. Kippelen, Appl. Phys. Lett. 97 (2010) 153304.

[27] C.X. Wang, G.W. Yang, T.C. Zhang, H.W. Liu, Y.H. Han, J.F. Luo, C.X. Gao, G.T. Zou, Diamond Relat. Mater.12 (2003) 1548.

[28] R.L. Hoffman, J.F. Wager, J. Appl. Phys. 90 (2001) 5763.

[29] M. Soylu, M. Girtan, F. Yakuphanoglu, Mater. Sci. Eng. B (2012), doi:10.1016/j.mseb.2012.03.025.

[30] G. Li, R. Zhu, Y. Yang, Nature Photonics 6 (2012) 153-161.

[31] L. Dou, J. You, J. Yang, C-C. Chen, Y. He, S. Murase, T. Moriarty, K. Emery, G. Li, Y. Yang, Nature Photonics 6 (2012) 180-185.

[32] H. Kim, J. Lee, SuperlatticesMicrostruct. 42 (2007) 255-258.

[33] D. Lee, D. Park, S. Kim, S. Y. Lee, Thin Solid Films 519 (2011) 5658-5661.

[34] H. Liem, H. S. Choy, K.C. Yung, Solid State Commun. 15 (2010) 1725-1728.

[35] S.M. Sze, *Semiconductor Devices*, 2nd ed. (Wiley, New York, 2001), p. 224.

[36] C. Sah, R.N. Noyce, W. Shockley, Proc. IRE 45 (1957) 1228.

[37] Y. Hirose, W. Chen, E.I. Haskal, S.R. Forrest, A. Kahn, Appl. Phys. Lett. 64 (1994) 3482.

FIGURE CAPTIONS.

Figure 1. FTIR-AT absorption spectra for an electropolymerized PEDOT layer onto an ITO/glass substrate from a 3 mM EDOT + 0.2 M $LiClO_4$ aqueous solution, by potential cycling from -0.8 to 2 V. Scan rate: 75mV/s and during 5 cycles.

Figure 2. FE-SEM images of PEDOT films grown under the experimental conditions given in Figure 1.

Figure 3. X-ray diffraction pattern of a typical RF magnetron sputtered ZnO thin film onto a PEDOT/ITO substrate. Hexagonal wurtzite ZnO JCPDS pattern is also shown for comparison (black lines). (*, indicates the peaks originated from the ITO substrate).

Figure 4. Cumulative optical transmittance spectra of a typical n-ZnO/p-PEDOT heterojunction diode onto an ITO/glass substrate. (a) glass; (b) ITO/glass; (c) PEDOT/ITO/glass and (d) ZnO/PEDOT/ITO/glass. The inset shows a photograph of a ZnO/PEDOT/ITO/glass diode device to illustrate its level of transparency.

Figure 5. (a) Schematic diagram of vertical n-ZnO/p-PEDOT heterojunction device. (b) The energy band diagram of the n-ZnO/p-PEDOT device and ITO and Al contacts.

Figure 6. (a) Current-voltage (I-V) characteristics of a typical n-ZnO/p-PEDOT hybrid heterojunction diode. The inset shows I-V characteristics of ITO/p-PEDOT ohmic contact. (b) I-V characteristics of the n-ZnO/p-PEDOT diode device in semilog form.

Tables (if any)

TABLE 1. Band assignments for the FTIR-AT absorption spectra of a PEDOT thin film shown in Figure 1.

Peak, (cm^{-1})	**Assigment and literature reported peak (cm^{-1})**		**Reference**
1523	ν(C=C)	(1515)	20
1475	ν(C-C)+ν(C=C)	(1450)	21
1412	ν(C-C)	(1388)	21
1363	ν(C-C)	(1334)	20
1221	ν(C-O-C)	(1202)	20
1145	ν(C-O-C)	(1141)	20
1095	ν(C-O-C)	(1090)	20
1054	ν(C-O-C)	(1050)	20
985	ν(C-S)	(979)	20
937	ν(C-S)	(945)	20
844	ν(C-S)	(844)	20

Figure1
Click here to download high resolution image

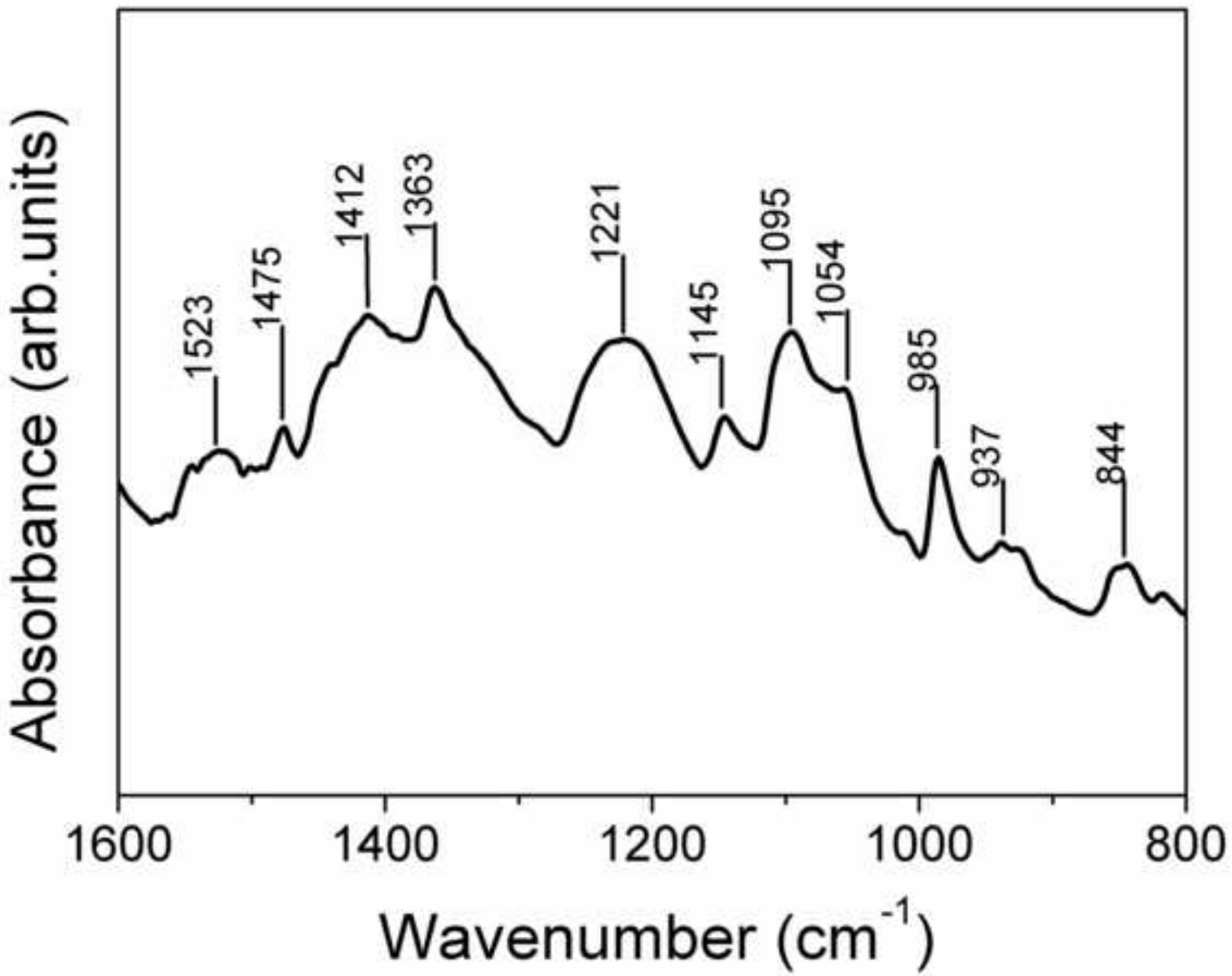

Figure2

Click here to download Figures (if any): Figure2.pdf

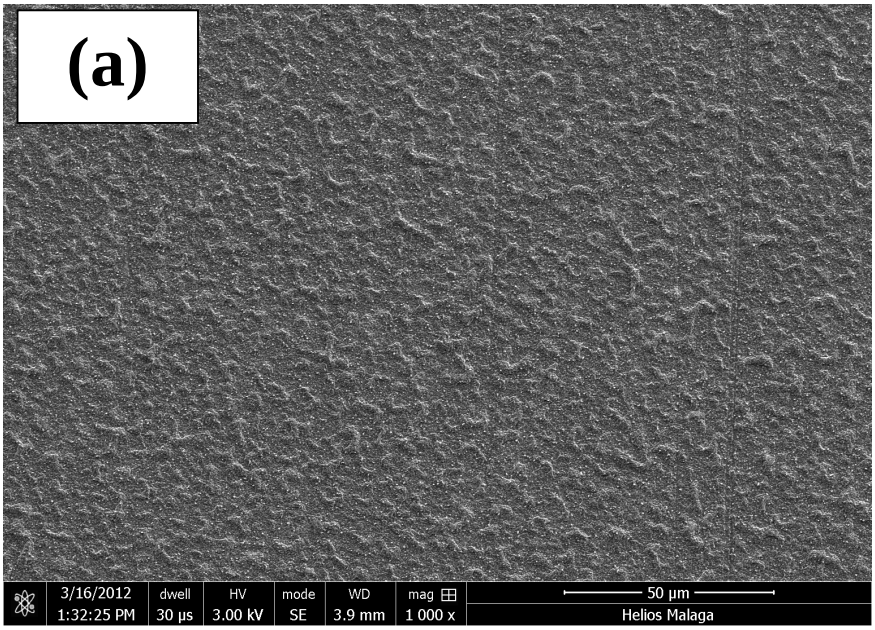

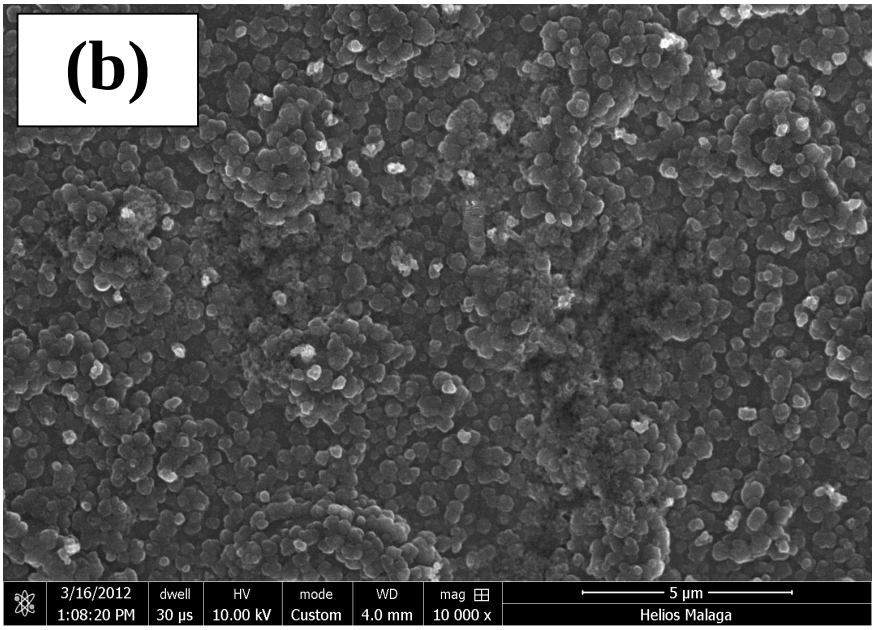

Figure3

Click here to download high resolution image

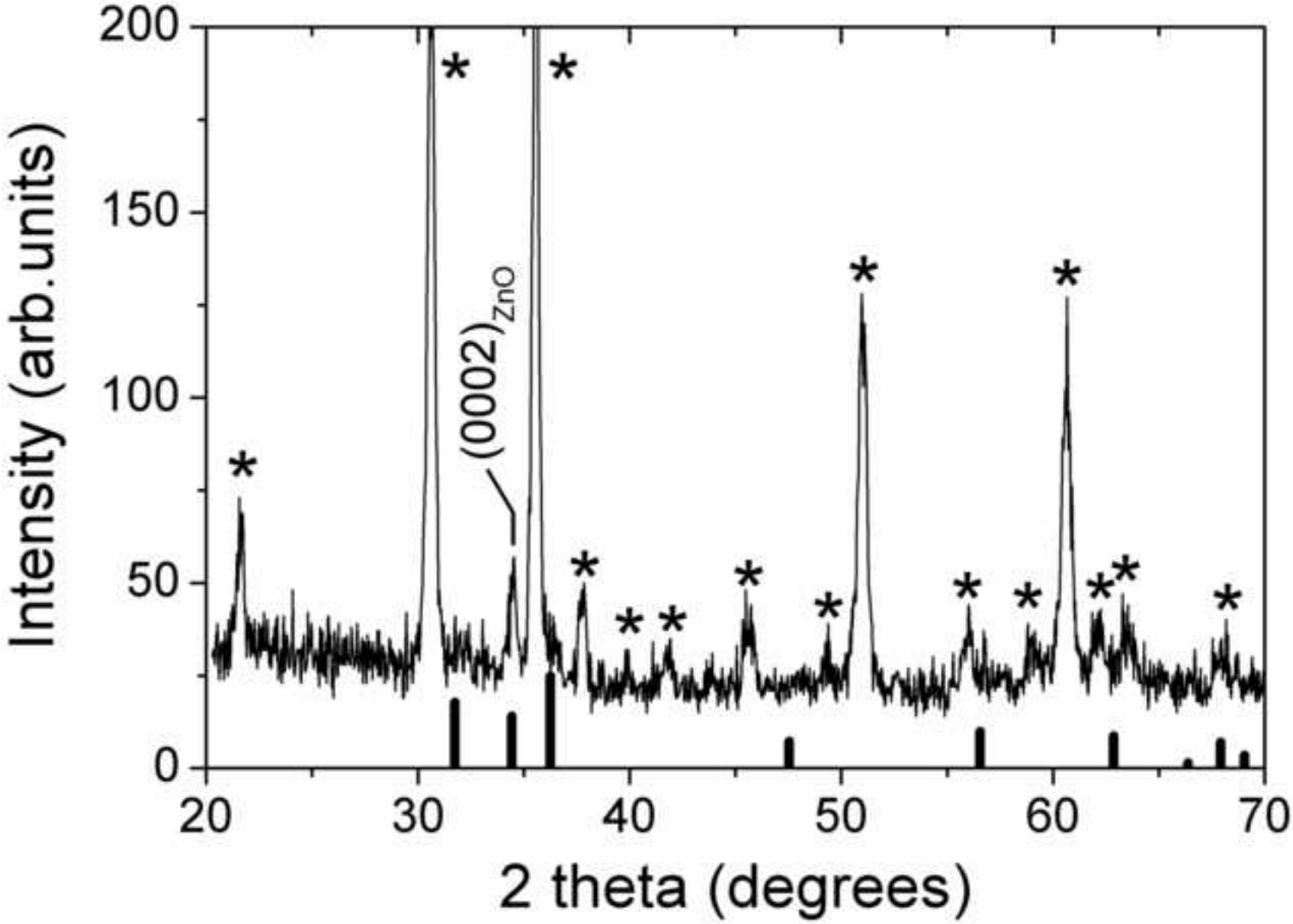

Figure4

Click here to download high resolution image

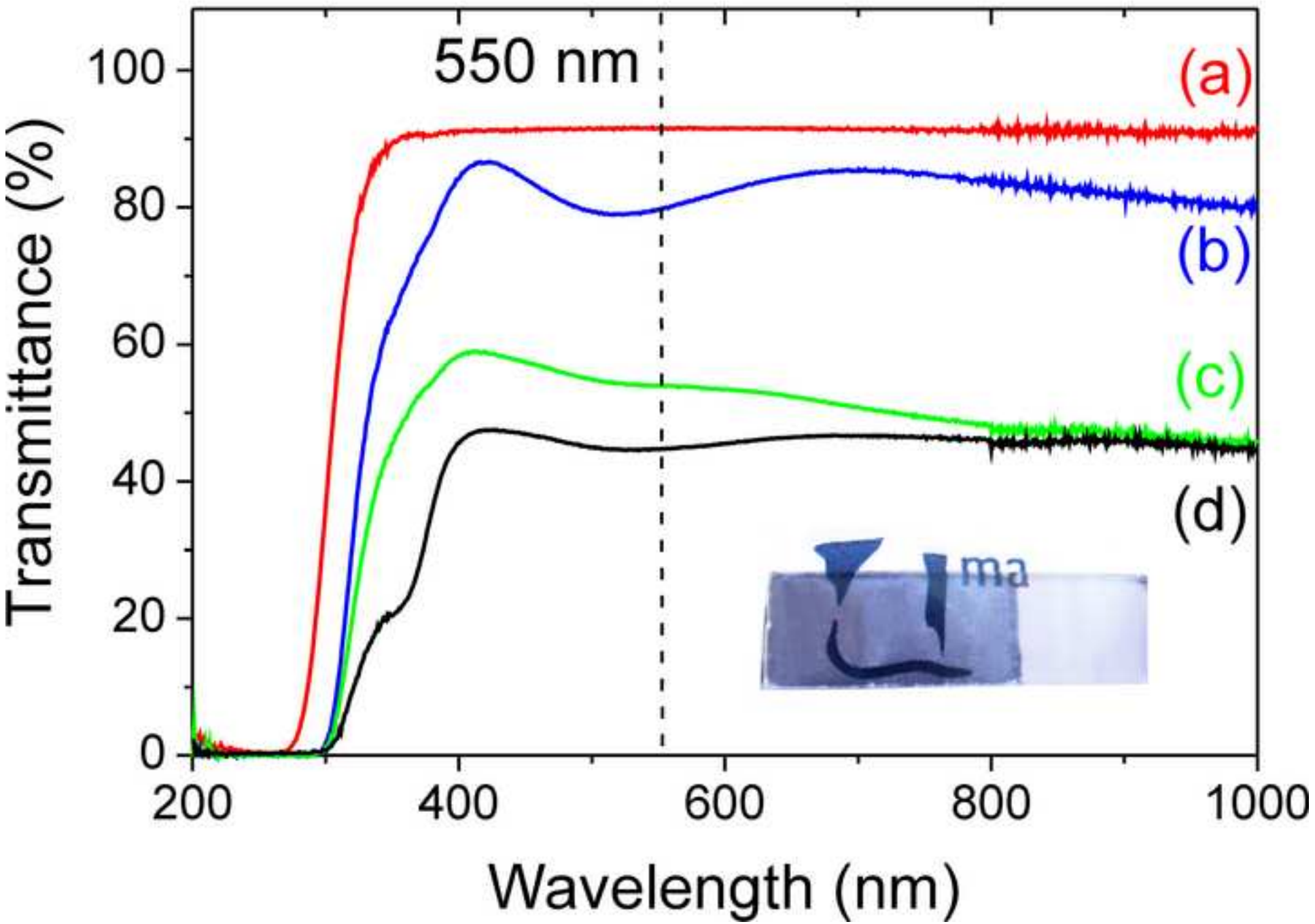

Figure5a
Click here to download high resolution image

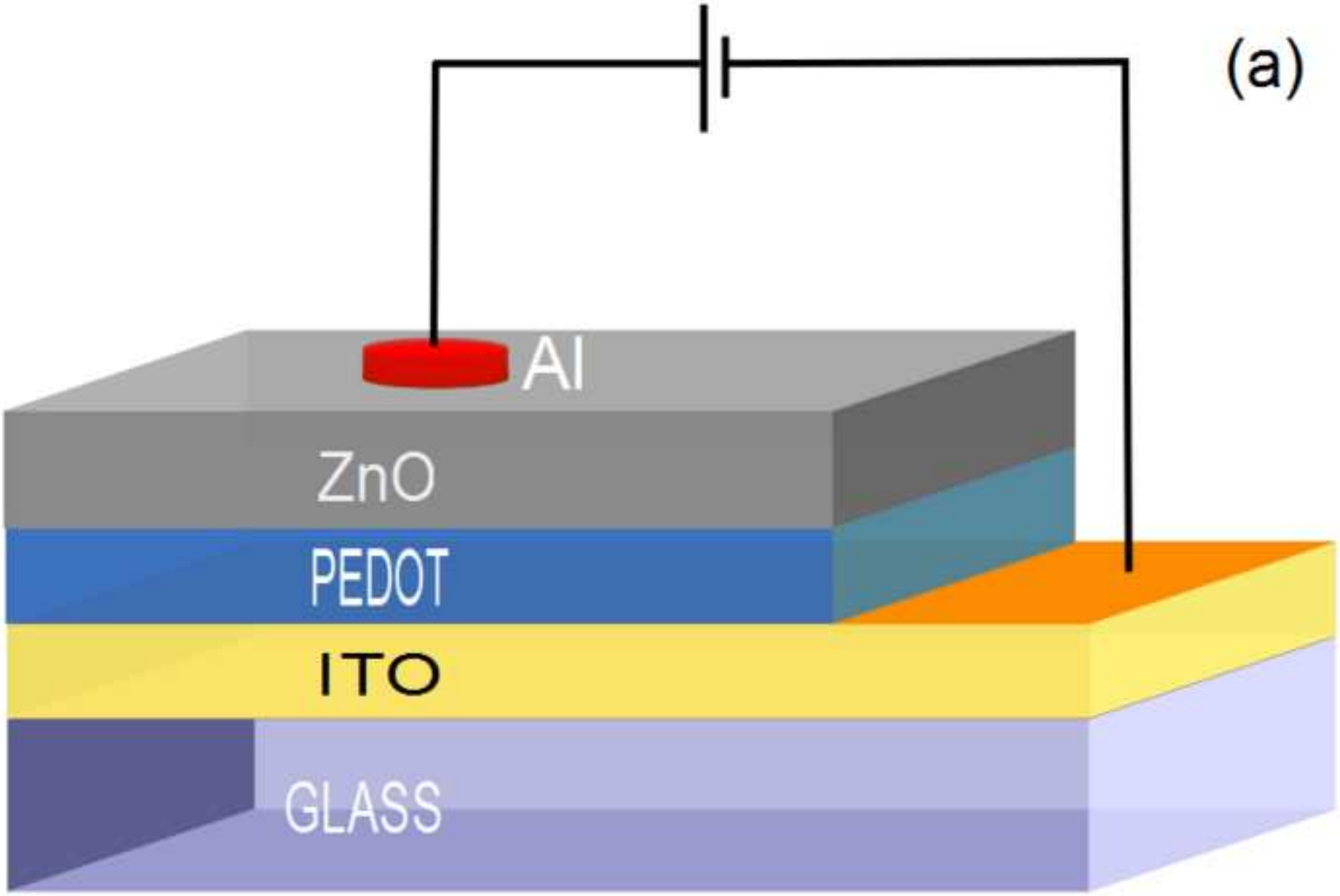

Figure5b

Click here to download high resolution image

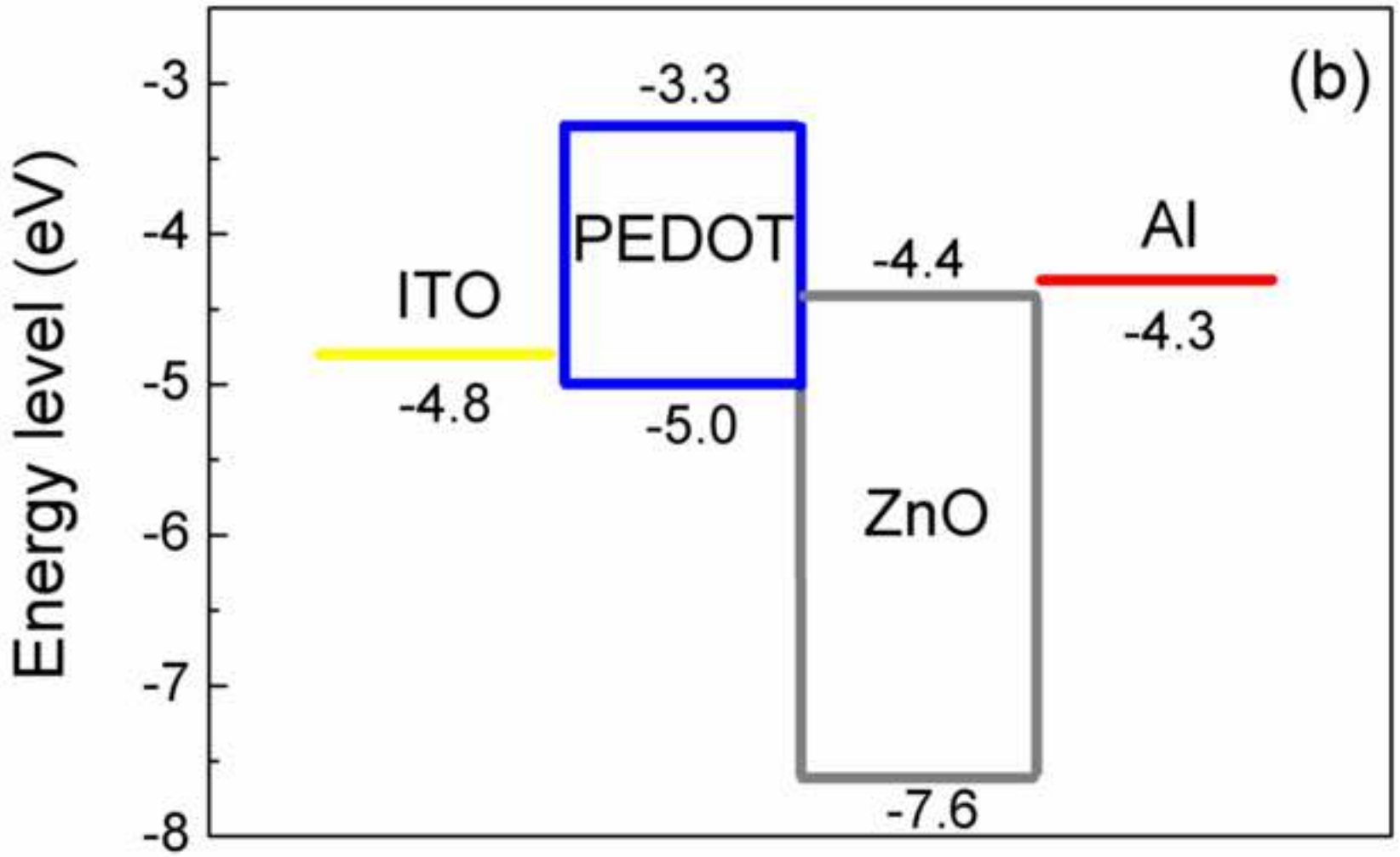

Figure6a

Click here to download high resolution image

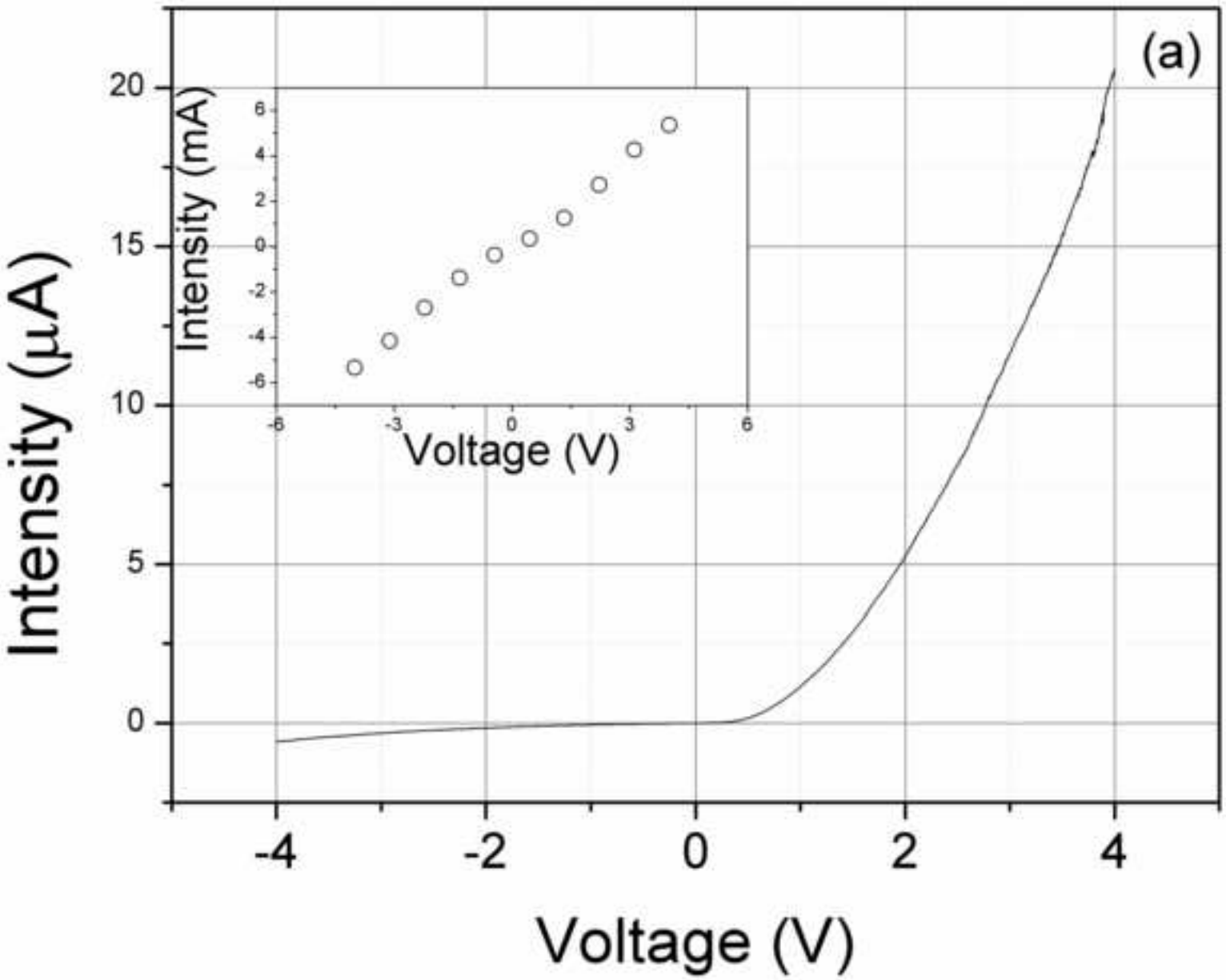

Figure6b

Click here to download high resolution image